# INVESTIGATION OF THE SUPERCONDUCTING PROPERTIES OF TRANSITION METAL ALLOY SYSTEMS

*final report to*

**NATIONAL AERONAUTICS AND SPACE ADMINISTRATION**

**UNDER CONTRACT NASw-733**



Arthur D. Little, Inc.

# INVESTIGATION OF THE SUPERCONDUCTING PROPERTIES OF TRANSITION METAL ALLOY SYSTEMS

FINAL REPORT

To

NATIONAL AERONAUTICS AND SPACE ADMINISTRATION

Under

Contract NAS w-733

C-65643

August 1964

Arthur D. Little, Inc.

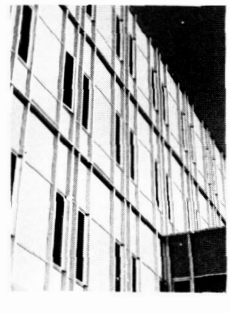

TABLE OF CONTENTS

## LIST OF FIGURES

## I. INTRODUCTION

17099 ABST

We have investigated the critical current characteristics of niobium-zirconium superconducting alloys. In particular, this study was concerned with the effect of the ω-transformation on superconductivity. This transformation has been studied in detail, and the purpose of this work was to apply this knowledge to the changes in superconducting properties as the transformation occurs.

AUTHOR

## II. EXPERIMENTAL METHOD

Zr-Nb alloys were prepared as described in the previous report,[1] and cut into strips about 10 mils x 10 mils x 1 inch. The alloy strips were then tinned with indium and loaded onto an abrasive wheel. The tinned ends were about 1/8 inch long. The tinned specimens were pressed into the indium current leads (Ref. 1, Fig. 1), and the leads were connected to the current-carrying copper wires.

Critical currents were measured as a function of applied transverse field. A superconducting type magnet with Nb-Zr windings was used to apply the field. This magnet, manufactured by Magnion, Inc., has an upper field of 28 kgauss. Current was supplied by a 0-10 V, 100 amp full-scale DC power supply. The applied field was held constant and current to the specimen was increased until a voltage drop was detected across the specimen. Voltage drop was measured across the center half inch of the wire with a Keithley microvoltmeter. The usual setting of the Keithley was 100 μV full-scale, so that it was possible to detect 0.2 μV changes. Little was gained from increasing the sensitivity of the microvoltmeter, since thermal emf's were also recorded, a difficult problem to overcome. Current, as measured by the voltage drop across a standard water-cooled resistance, and voltage, from the amplified output of the Keithley microvoltmeter, were recorded on a Mosley X-Y recorder. Once the technique was developed, it was extremely reproducible; however, some difficulties had to be overcome.

The major obstacle was the fluctuations in the voltage response on the X-Y recorder. As the current was increased, the voltage trace would start to oscillate on both sides of the zero voltage line. As current was increased still more, the frequency of the oscillations increased and further maxima in the oscillations occurred at particular current levels. As the applied field was increased, the maximum amplitude of the oscillations decreased, and usually the superconducting transition would be obscured completely. The fact that a

negative voltage drop occurred was sufficient proof that the oscillations were spurious, but they were, nevertheless, difficult to remove. At first, electronic breakdown of the voltage amplifier or recorder was suspected, but the problem was found to be elsewhere. When the voltage outputs were connected to an oscilloscope, the specimen acted as an oscillator, although the response on the oscilloscope showed little relation to that of the recorder. (Apparently the DC microvoltmeter could not handle the millisecond voltage oscillations from the specimen, and the output on the recorder was not representative of the true signal.) The explanation for the oscillations is that the superconducting specimen and parallel shunt combination acted as a relaxation oscillator. The copper shunt was placed in parallel with the specimen to lower the current through the specimen when the specimen became resistive to prevent it from burning out. However, whenever current was diverted from the specimen to the shunt, the specimen would become superconducting again and cause the cycle to repeat. Thus, the voltage drop across the specimen oscillated. An attempt was made to remove the oscillations by changing the resistivity of the copper shunt, but the oscillations were still evident as long as the shunt was present.

To stop the voltage oscillations from the specimen, the shunt had to be removed. This meant another way had to be found to prevent the specimen from burning out when it became resistive. A switching system was constructed to cut off the current to the specimen as soon as a 100 $\mu$V voltage drop was detected across the potential leads. The signal was amplified and used to operate a mechanical relay, but the total switching time (10 milliseconds) from finite to zero current was too long to prevent burnout. Instead of using a mechanical relay, we constructed the current stop circuit described below and built it into the power supply. The switching time was then 0.4 millisecond. The design of the power supply was also changed to that shown in Figure 1.

The power supply consists of a series-shunt voltage-regulated circuit. The variable output voltage is controlled by a constant voltage source consisting of $CR_eQ_6$, and $R_1$ in the reference supply. The output control is ganged to a variable input transformer, $T_i$, to set a low collector-to-emitter voltage of the output transistors. The output transistors consist of nine parallel power transistors to allow large load currents without exceeding the transistor power rating. A small resistor, $R_n$, is placed in series with each base, which equalizes the emitter currents of the output transistors.

As the transition from the superconducting state to the normal state of the sample under test occurs, the sensor (-A) generates a trigger pulse which resets the power supply by means of the current-stop circuit.

The trigger pulse, generated by the -A sensor, is coupled to $Q_1$; it is inverted, amplified, and coupled through $C_3$ to $Q_5$, switching it into its saturated mode and thereby resetting the power supply in 0.4 millisecond. However, with

an inherent relay delay of 10 milliseconds, the supply will turn itself back on before $K_1b$ can switch, holding the supply off. Therefore, capacitor $C_1$ is placed across the input of the current-stop circuit and charged through $CR_1$. Hence, when the sample goes normal, the sensor (-A) will generate a trigger pulse and charge $C_1$ through $CR_1$. Upon removal of the trigger pulse because of cutback in sample current, $CR_1$ becomes back-biased so that the discharge time-constant $C_1R_n$ is approximately 50 milliseconds, holding $Q_1$ in its saturated state and allowing sufficient time for $K_1b$ to switch, holding the supply in its off state until the reset circuit is activated. $Q_4$ and $K_2$ are used as a remote pen left control for recording.

The "critical current vs applied transverse field" curves were obtained for various zirconium alloys which show the ω- transformation. The alloys studied were zirconium-based with 15, 20 and 30 atomic percent niobium. Two heat treatments were used; in one, designated the C series, alloy sheet was heat-treated at 920°C for 24 hours in evacuated quartz tubes. The specimens were water-quenched and rolled to 13% of the original thickness. They were then further heat-treated in evacuated quartz tubes at 920°C for 2 hours to anneal the sheet and to solution-treat it in the ω-phase region. The alloy was then water-quenched. The second heat treatment, designated the B series, was similar, except after cold rolling the specimens were not heat-treated at 920°C again. For both the B and C series, specimens were further heat-treated at 400°C for various times. In the 400°C heat treatment both the amount and structure of the ω-phase will change with time. Critical current as a function of field is plotted for the three alloys in Figures 2 through 7. Table 1 lists the figure numbers for the various alloy contents as well as the series designations.

TABLE 1

FIGURE NUMBERS OF THE CRITICAL CURRENT VS FIELD CURVES FOR THE ZIRCONIUM-NIOBIUM ALLOYS

| ALLOY (at % Nb) | SERIES | FIGURE NUMBER |
|---|---|---|
| 15 | C | 2 |
| 15 | B | 3 |
| 20 | C | 4 |
| 20 | B | 5 |
| 30 | C | 6 |
| 30 | B | 7 |

## III. EXPERIMENTAL RESULTS

It can be seen from Figures 2-7 that the form of the curves of critical current density (J) vs transverse field (H) is very sensitive to heat treatment. Considering the C series first, Figures 2, 4, and 6, it can be seen that the quenched specimens show a rapid drop of J with increasing H for the three alloys. As the specimens are heat-treated for various times at 400°C, the curves show increasingly higher values of J at the upper fields. The effect of heat-treating time at 400°C on the value of J at a field of 20 kgauss for the 15 at % Nb alloy can be seen in Figure 8, and on the 30 at % Nb alloy in Figure 9. The form of the curves is identical in Figures 8 and 9. Note from the B series of J vs H curves (Figures 3, 5 and 7) that cold working the alloys prior to deformation affects the J vs H curves. It can be seen from Figures 8 and 9 that cold work prior to deformation reduces the aging time of the alloys necessary to cause the highest values of J at H = 20 kgauss. If one compares the two J vs H curves for the alloys in the as-quenched and the as-rolled conditions (Figures 2 and 3, 4 and 5, 6 and 7) one sees the influence of cold work on these curves. At the higher fields, J is increased by cold work. Cold work of the Zr-Nb alloy accelerates the 400°C reaction products which change the J vs H curves.

The flat J vs H curves that occur, for example, the upper curve in Figure 2, are probably a result of contact resistance at the current leads to the specimen. Ralls et al[2] and Heaton and Rose-Innes[3] report that if contact resistance is present, the apparent critical current is nearly independent of applied magnetic field. At higher critical fields, heating at the current contacts causes the premature transition from superconducting to normal because of nucleation. No doubt, the flat curves should show higher critical currents than indicated. It is still possible to observe qualitatively the effect of heat treatment of the alloys on their J vs H curves. Despite efforts to reduce the contact resistance by further refinements of the abrasive tinning techniques and by methods described by Ralls et al[2], no significant improvement was noted.

The highest current densities obtained at a field of 20 kgauss for each of the alloys is given in Figure 10. Note that the maximum value of J occurred for the 30% alloy, which has a J value about 4 times greater than that of the 15% Nb alloy. If the contact resistance were eliminated, the effect of alloy content on the maximum value of J at H = 20 kgauss would probably be greater than that noted.

## IV. DISCUSSION

The observed results will be discussed in view of the known information about the ω-transformation in the zirconium-rich niobium alloys. Zirconium shows a phase transformation from body-centered-cubic to close-packed-hexagonal. Alloys in the composition range studied consist of a single body-centered-cubic phase $\beta$ at 920°C; at room temperature the alloys consisted of two phases in equilibrium: a zirconium-rich close-packed-hexagonal one and a niobium-rich body-centered-cubic one. The quenched alloy contains an intermediate phase ω that forms without either composition change and retained $\beta$. The metastable ω-phase is hexagonal, and is an intermediate structure between BCC and CPH. The ω-phase which first forms is highly faulted and has been designated diffuse ω by Hatt and Roberts[4]. If the specimen is heated at 400°C, the ω-phase becomes less diffuse; in other words, the faults tend to anneal out. Since diffusion can occur at this temperature in reasonable times, the compositions of the $\beta$ and ω phases change. The increase of the critical current curves with holding times of the alloys at 400°C is probably similar in nature to the effect on reversibility of magnetization curves in precipitation alloys as seen by Livingston[5]. Lead base superconducting alloys showed less magnetic hysteresis in the as-quenched condition than when they had a cellular precipitate. Trapping of flux depended upon the size and distribution of the second phase. It can be seen from Figure 2 in the paper by Heaton and Rose-Innes[3] that an increase of magnetic hysteresis is indicative of an increase in the ability of an alloy to carry higher currents in field before becoming normal. The quenched alloys must show small trapping of flux. The diffuse ω-phase which exists must be close to the $\beta$ matrix in structure to make the alloys appear as a homogeneous alloy. As the alloys are heat-treated at 400°C, the ω-phase probably increases in amount and becomes less faulted. The alloy becomes less homogeneous, and the amount of flux trapped increases. Over-aging can occur (see Figure 8) just as in age-hardening of alloys. If the alloy is aged for too long a time, the distribution of the second phase and the size of the second phase particles must be such that the alloy goes through a maximum in the critical currents carried at the higher fields.

It would be of value to determine the magnetization curves of one of these alloys to find the effect of heat treatment on the reversibility of the magnetization curves. Higher fields are needed to determine both the upper critical field magnetically and resistively. To obtain higher fields, facilities at the MIT National Magnet Laboratories would be used.

## REFERENCES


1. Second Quarterly Report to National Aeronautics and Space Administration NASw-733.

2. K. M. Ralls, A. L. Donlevy, R. M. Rose and J. Wulff, Report No. 149, Department of Metallurgy, Massachusetts Institute of Technology.

3. J. W. Heaton and A. C. Rose-Innes, Cryogenics, 4, April 1964, p. 85.

4. B. A. Hatt and J. A. Roberts, Acta Metallurgica, 8, 1960, p. 575.

5. J. D. Livingston, Physical Review, 129, 1963, p. 1943.

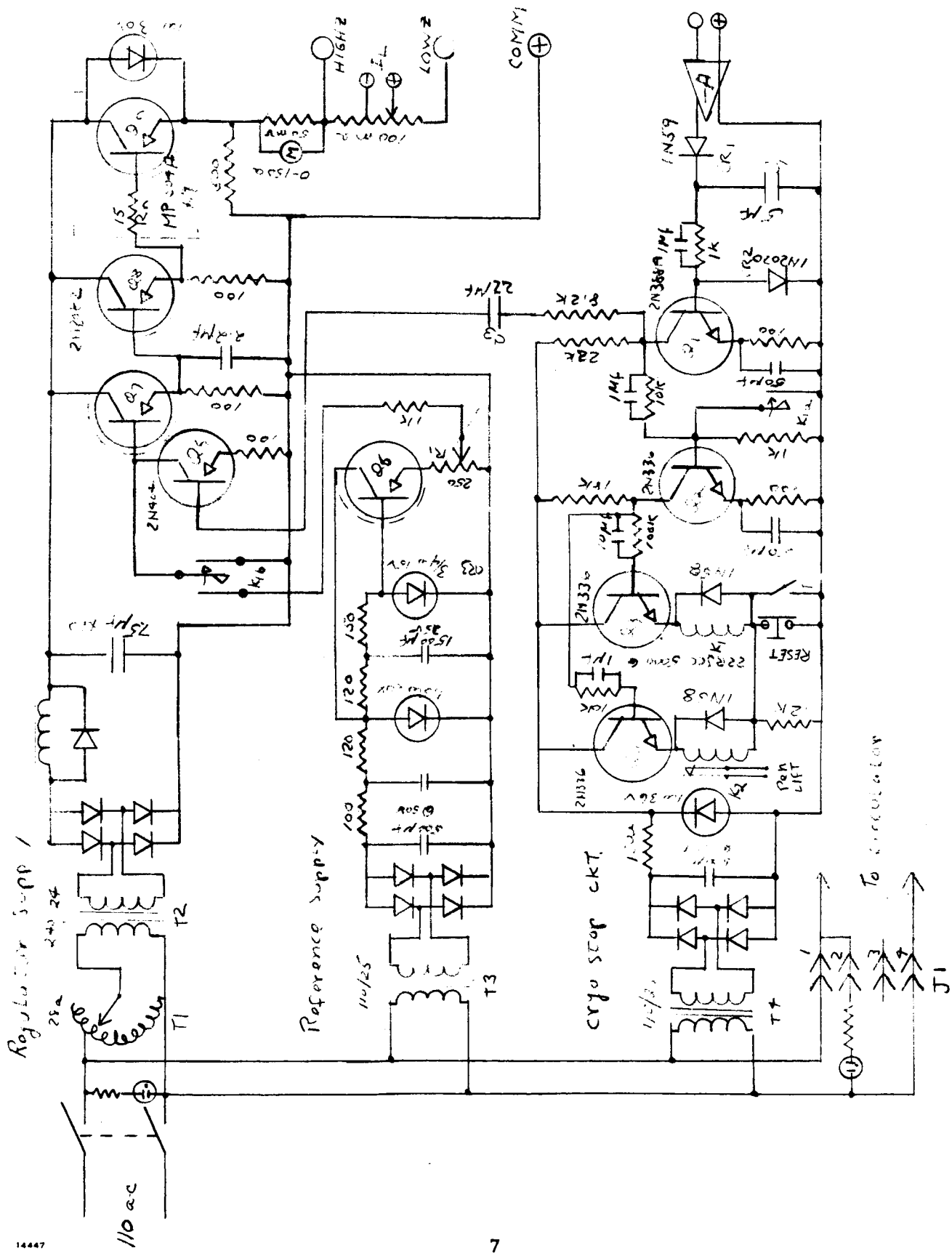


FIGURE 1 0-10 VOLT, 100 AMP POWER SUPPLY AND CURRENT STOP

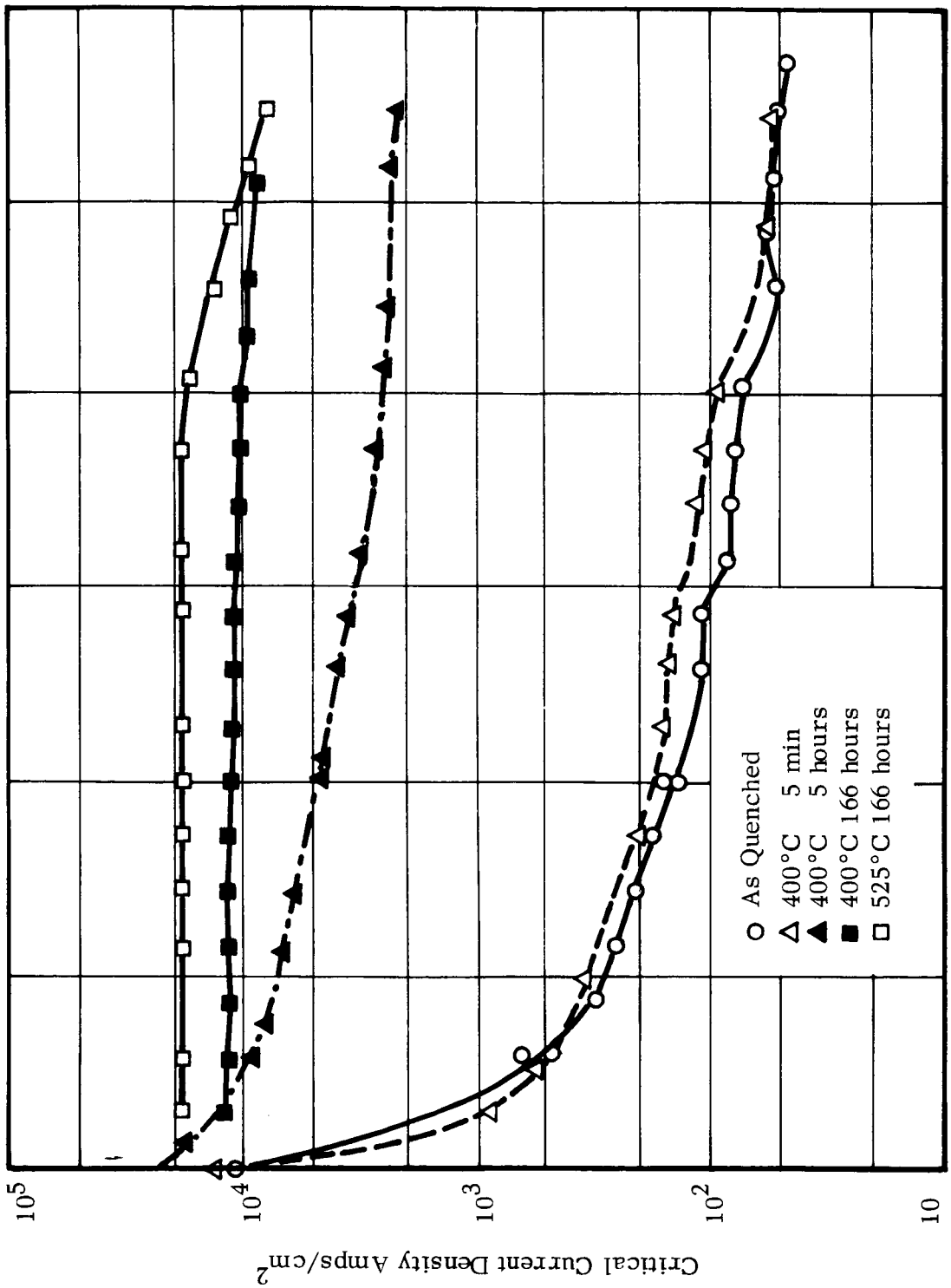


FIGURE 2 CRITICAL CURRENT DENSITY VS FIELD FOR C SERIES OF THE Zr-15 AT % Nb ALLOY

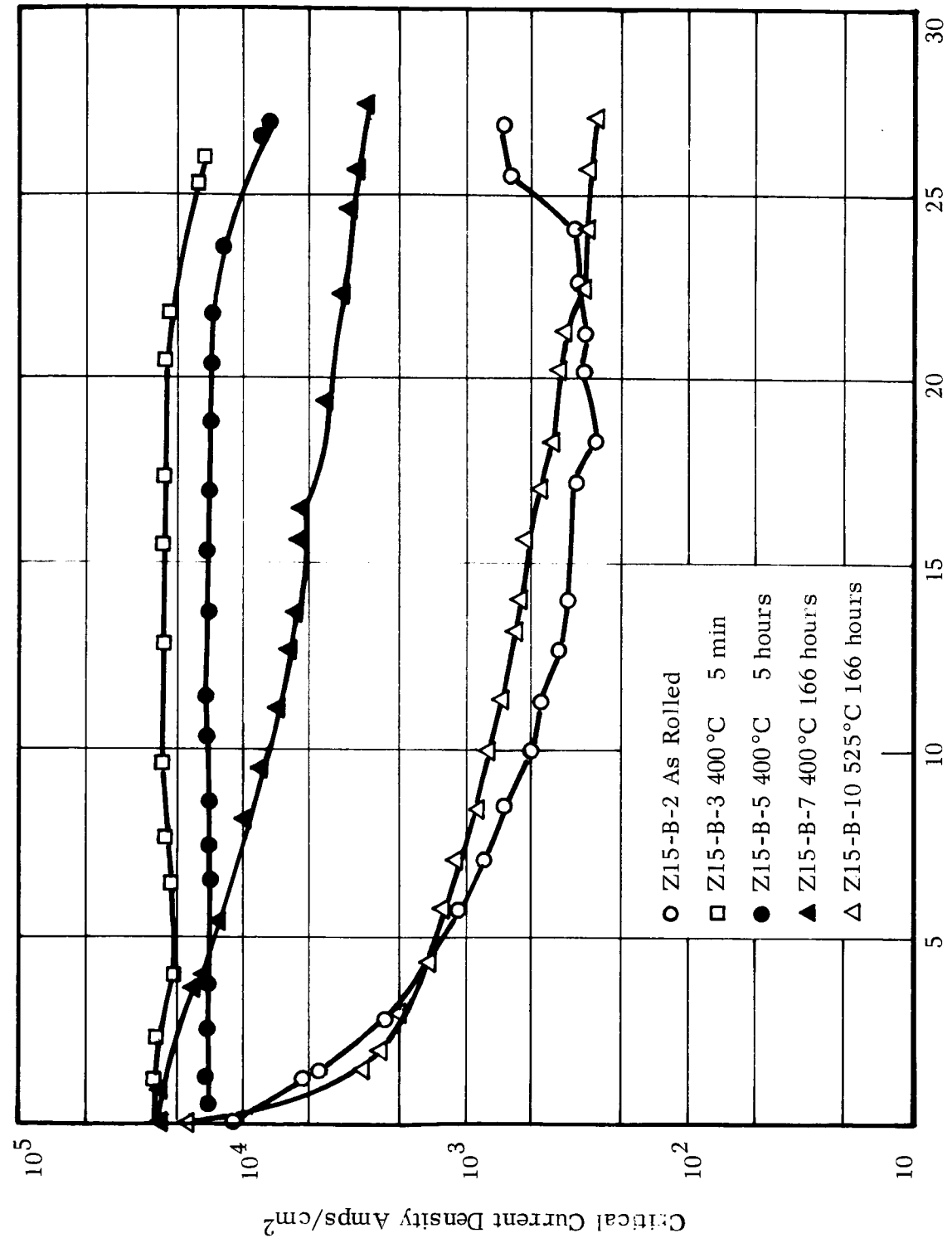


FIGURE 3 CRITICAL CURRENT DENSITY VS FIELD FOR B SERIES OF Zr-15 AT % Nb ALLOY

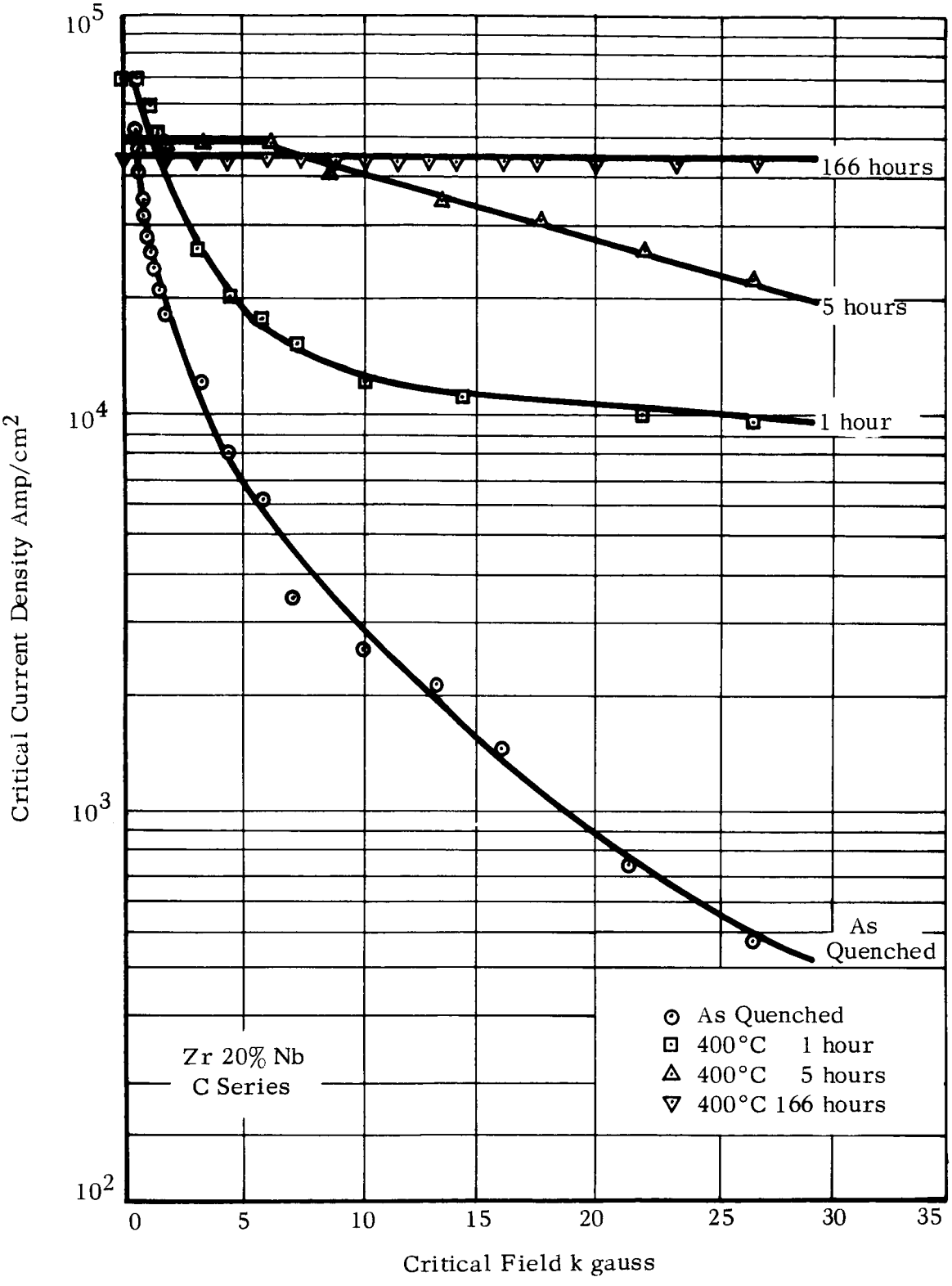


FIGURE 4 CRITICAL CURRENT DENSITY VS FIELD FOR C SERIES OF Zr-20 AT % Nb ALLOY

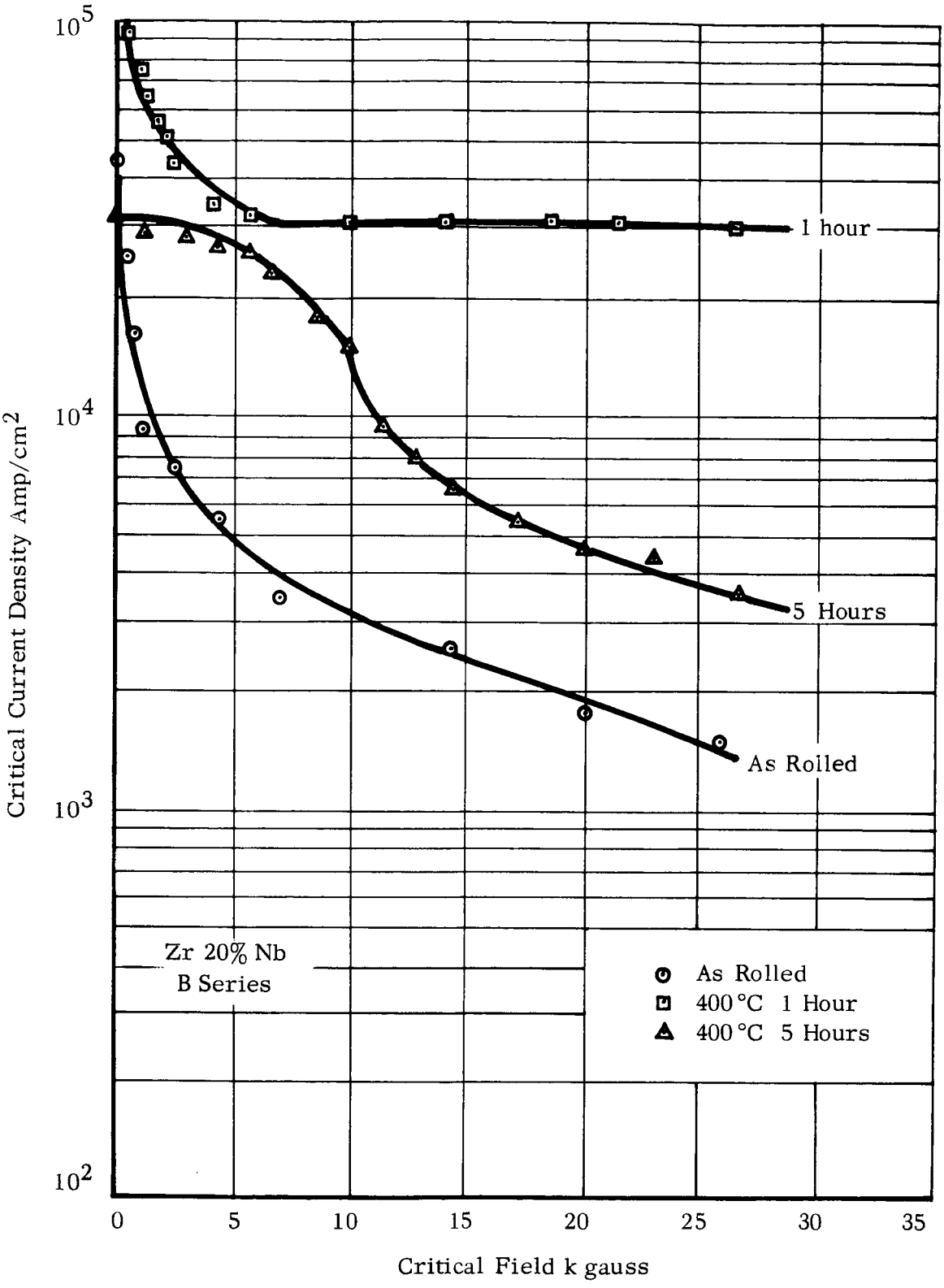


FIGURE 5 CRITICAL CURRENT DENSITY VS FIELD FOR B SERIES AT Zr-20 AT % Nb ALLOY

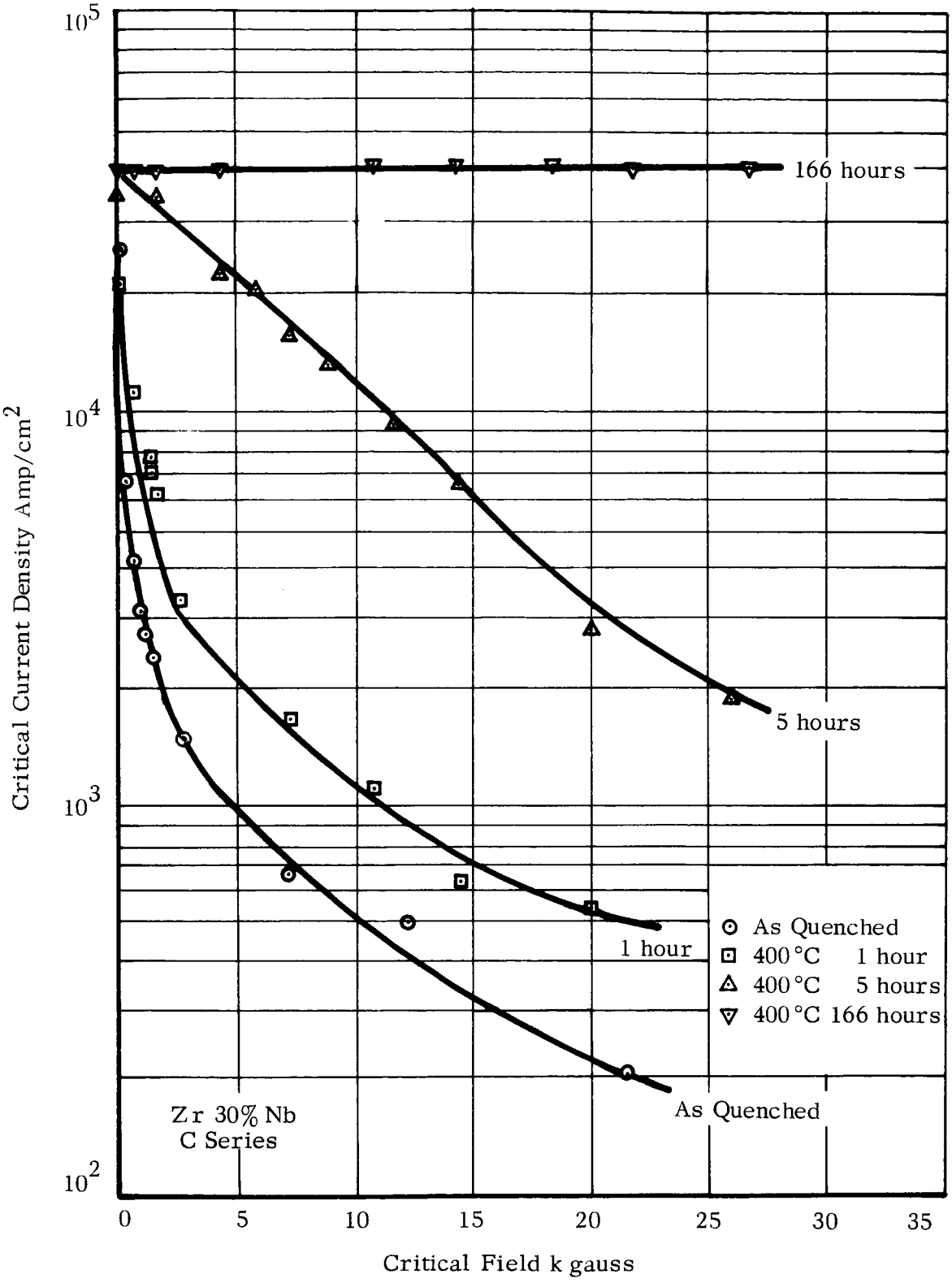


FIGURE 6 CRITICAL CURRENT DENSITY VS FIELD FOR C SERIES OF Zr-30 AT % Nb ALLOY

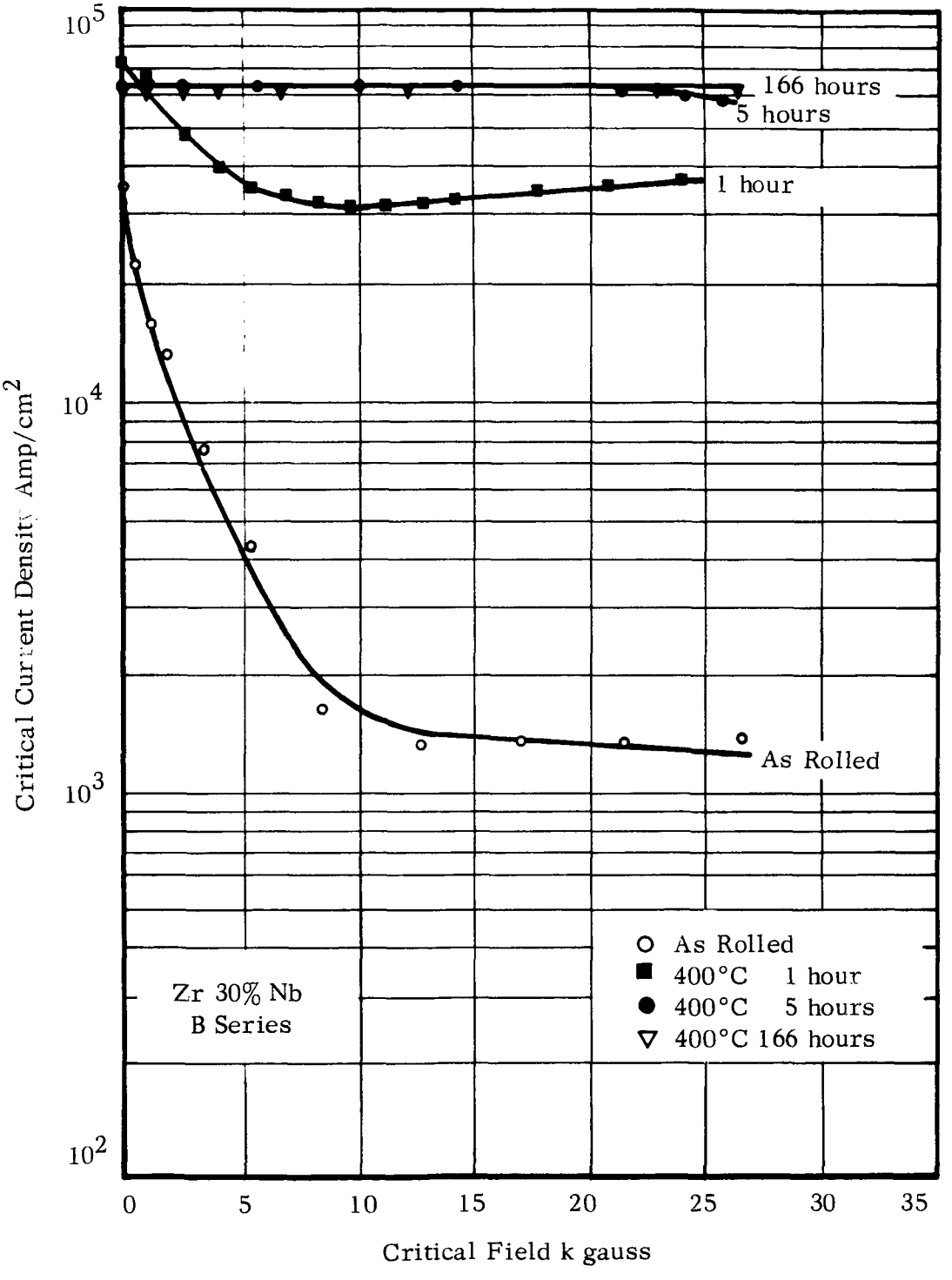


FIGURE 7 CRITICAL CURRENT DENSITY VS FIELD FOR B SERIES OF Zr-30 AT % Nb ALLOY

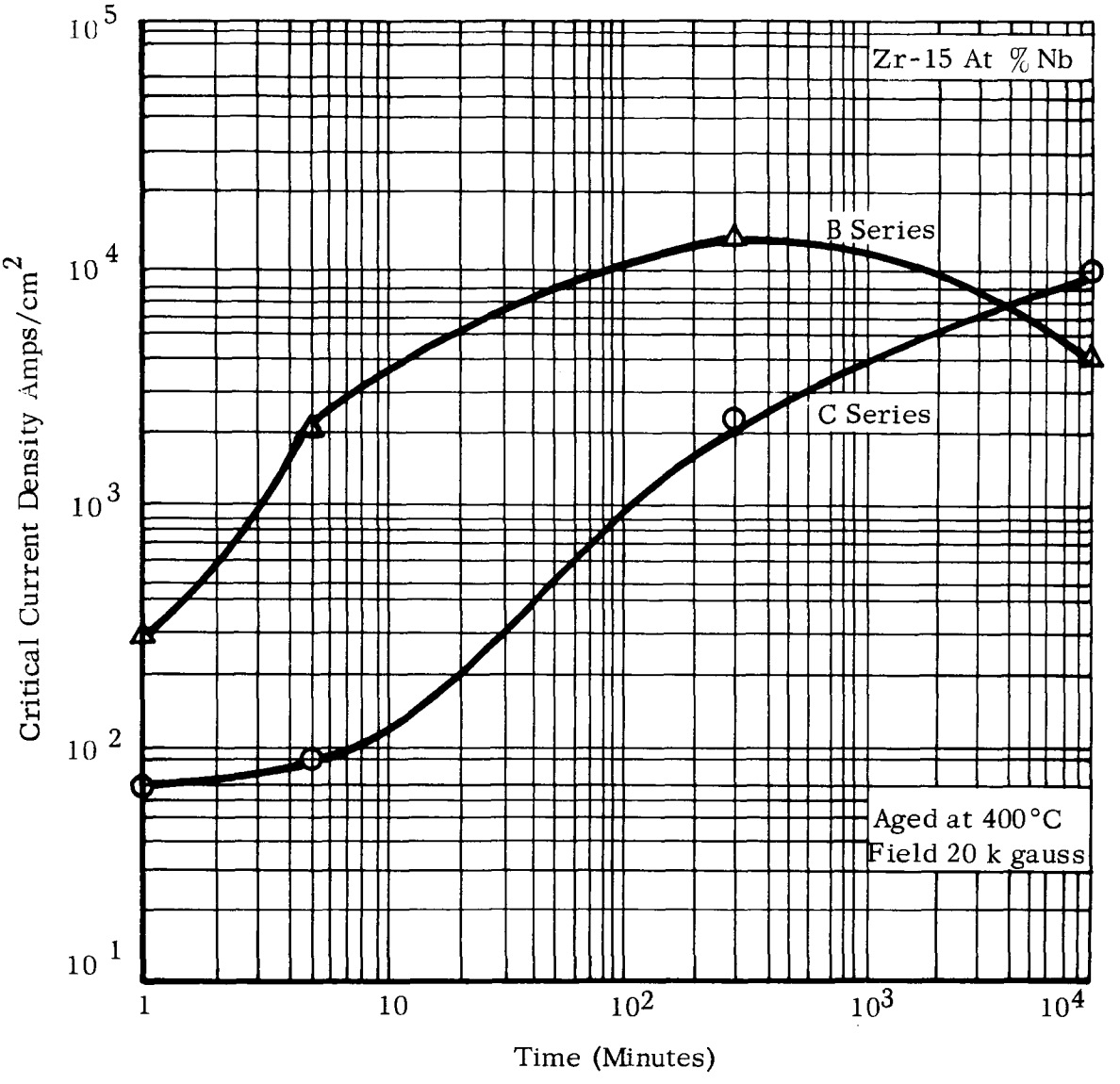


FIGURE 8 CRITICAL CURRENT DENSITY VS AGING TIME AT 400°C FOR B AND C SERIES OF THE Zr-15 AT % Nb ALLOY

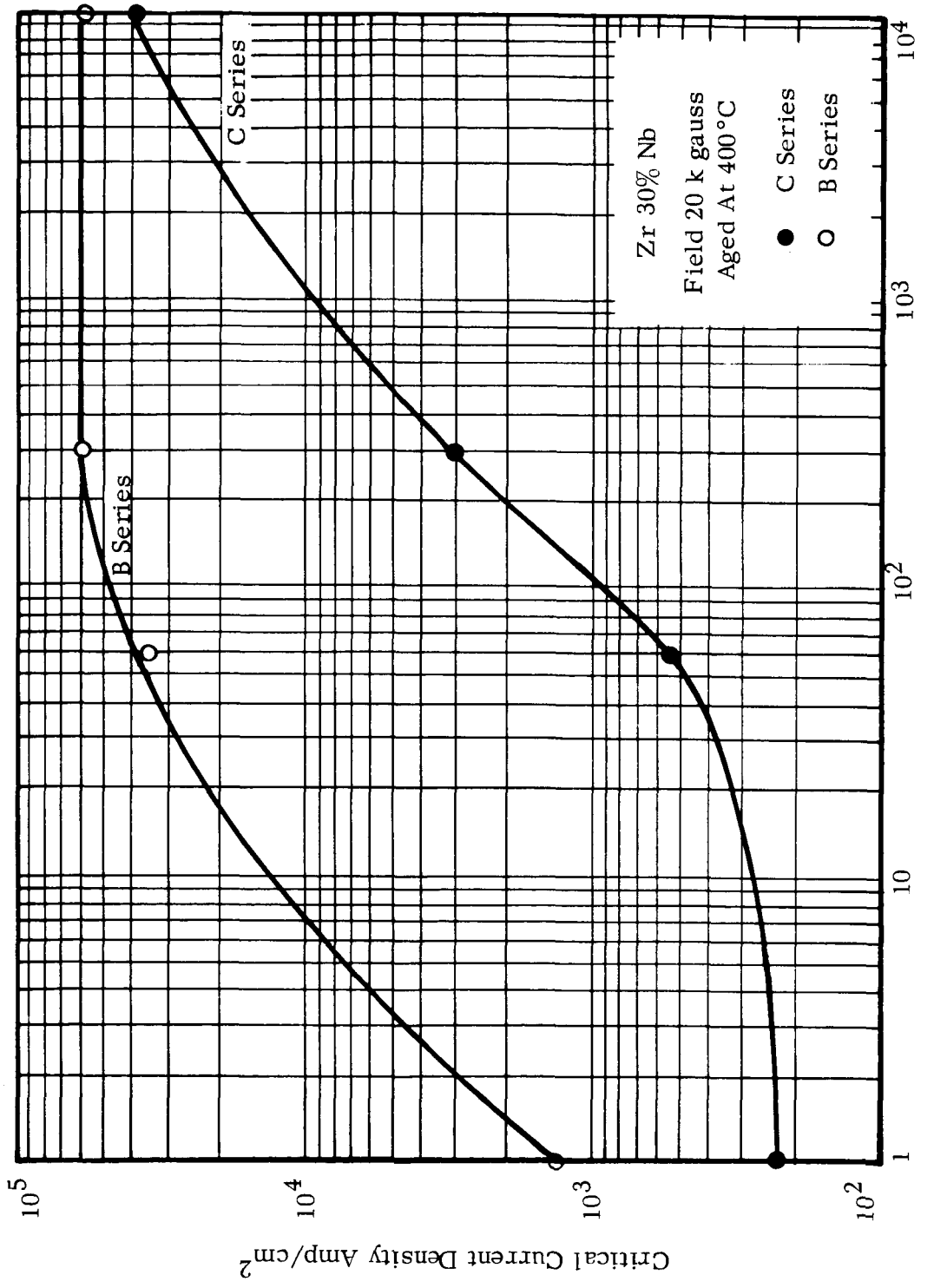


FIGURE 9 CRITICAL CURRENT DENSITY VS AGING TIME AT 400°C FOR B AND C SERIES OF Zr-30 AT % Nb ALLOY

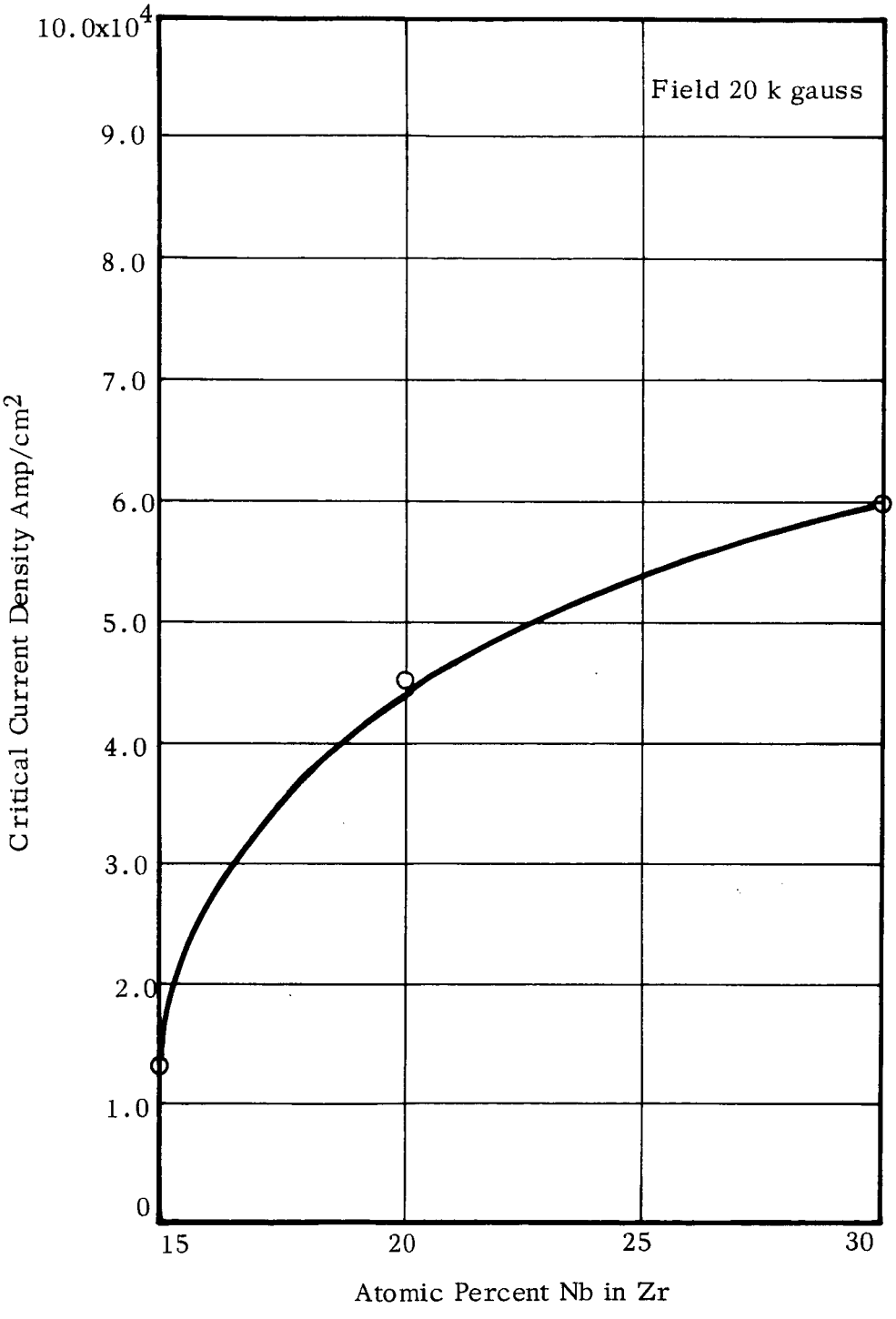


FIGURE 10 EFFECT OF COMPOSITION ON HIGHEST CRITICAL CURRENT DENSITY IN Zr-Nb ALLOYS AT A FIELD OF 20 k gauss